Spin Injection and Transport in Oxide Semiconductors

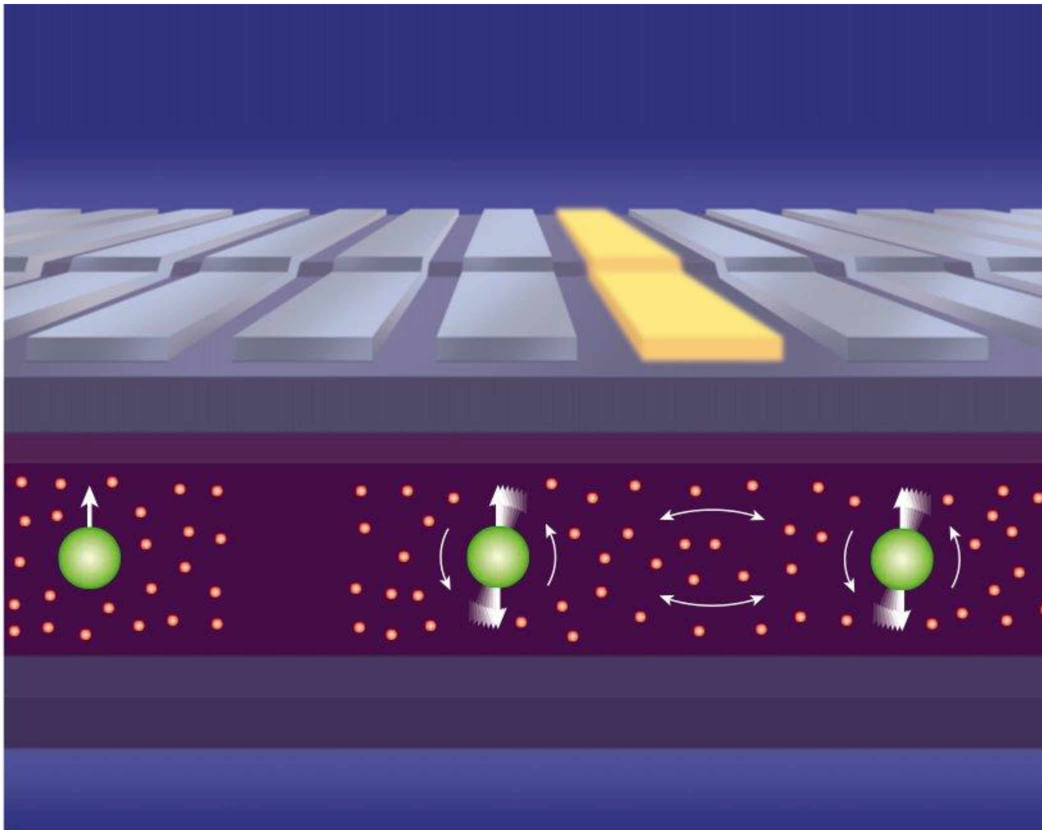

SAMPSON ADJOKATSE

(S2300664)

Topmaster in Nanoscience

Zernike Institute for Advanced Materials

August, 2014

ABSTRACT

Oxide materials exhibit a wide range of functional properties that make them important in technological applications. For instance, the transport properties of oxides span from superconductivity to high-mobility metallicity, semiconducting properties and insulating behaviour. Thus, a single oxide material has the ability to exhibit the characteristics of a memory and at the same time, the properties of semiconductors and insulators. In this paper, we present a systematic review of spintronic devices based on semiconductors. We then focus on oxide semiconductors and present an extensive study into the phenomenon of spin injection, relaxation and detection in this category of oxide materials. In particular, we study the spin injection and transport in $La_{0.7}Sr_{0.3}MnO_3$ (LSMO)/Nb-doped $SrTiO_3$ (Nb:STO) device.

Table of Contents

ABSTRACT 2
1 INTRODUCTION 4
2 SEMICONDUCTORS FOR SPINTRONICS 5
3 OXIDES FOR SPINTRONICS 6
3.1 Magnesium Oxide (MgO) 6
3.2 Strontium Titanate ($SrTiO_3$) 8
3.3 Lanthanum Strontium Manganate (LSMO) 9
4 BASIC ELEMENTS OF SPIN INJECTION AND TRANSPORT 9
4.1 Spin Injection and Detection 10
4.2 Spin transport 11
5 SPIN INJECTION AND TRANSPORT IN OXIDE SEMICONDUCTORS 12
6 CONCLUSION 14
REFERENCES 16

1 INTRODUCTION

An important driving force in information technology is the growing concern about future generations of electronic circuits. The rapidly increasing power consumption and heat generation of electronic circuits limit the operating speed of semiconductor chips to below the capabilities of the individual transistors. This shows a clear need for alternatives that can add to, extend or even replace existing technology. The integration of magnetic materials and impurities into nanoelectronic devices enables the use of the electron spin as well as its charge for processing and storing information. This new paradigm in information processing devices is called spintronics, in analogy to electronics. It involves the study of the role played by electron (and more generally, nuclear) spin or the active control and manipulation of spin degrees of freedom in solid-state systems.

The emergence of this field is linked to the discoveries in the 1980s concerning spin-dependent electron transport phenomena in solid-state devices. These include the observation of spin-polarized electron injection from a ferromagnetic metal to a normal metal by Johnson and Silsbee [1] and the discovery of giant magnetoresistance (GMR) independently by the team of Albert Fert [2] and Peter Grunberg and co-workers [3]. After this ground-breaking discovery, large varieties of spintronic effects have been observed and studied [4] including tunneling magnetoresistance (TMR) effects. However it is important to note that the origin of spintronics can be traced back even further to the ferromagnet/superconductor tunneling experiments pioneered by Meservey and Tedrow [5], and initial experiments on magnetic tunnel junctions (MTJs) by Julliere in the 1970s [6].

There are two main categories of spintronics devices, passive and active. Passive spintronic devices make use of the spin degrees of freedom, whereas active spintronic devices employ both the spin and charge degrees of freedom. While the net polarization of the spins in a material is used for data storage and retrieval, active spintronic devices rely on manipulation to generate versatile devices with the capabilities of both traditional electronics and passive spintronics. The discoveries of GMR and TMR effects and their subsequent applications led to phenomenal impact in data storage and information processing in electronic technology. An example is metal-based spintronics which has transformed magnetic data storage and memory applications through giant and tunnel magnetoresistance in layered magnetic structures [7-9]. Metallic spintronic devices, such as hard disk read heads and magnetic random access memory (MRAM) are some of the most successful technologies with scaling trends outdoing complementary metal-oxide-semiconductor (CMOS) technology.

However, in spite of the significant impacts of metallic spintronic devices, they are limited in various ways. One such limitation is in signal amplification, a property required to enhance device functionality [10]. This has led to worldwide efforts to integrate semiconductors and magnetic materials to create a revolutionary and energy-efficient information technology in which digital data are encoded in the spin of electrons [11]. In principle,

ferromagnets have non-volatile memory functionality at ambient temperature and their magnetization can be switched rapidly and with unlimited endurance. On the other hand, the properties of semiconductors can be controlled by doping (density and type), by light and by electrostatic gates, providing amplification and transistor action. Bandgap engineering also allows one to build various low-dimensional heterostructures. Thus, the combination of ferromagnets and semiconductors goes beyond the impacts of metal-based spintronics, exploiting the unique features that make both of these materials so successful and guided by the "create, manipulate and detect" principle [11] (see Figure 1). This alternate variant to metallic spintronics referred to variously as semiconductor-based spintronics or simply as semiconductor spintronics is briefly discussed below. Another significant stride that is also discussed is the use of oxides in spintronics.

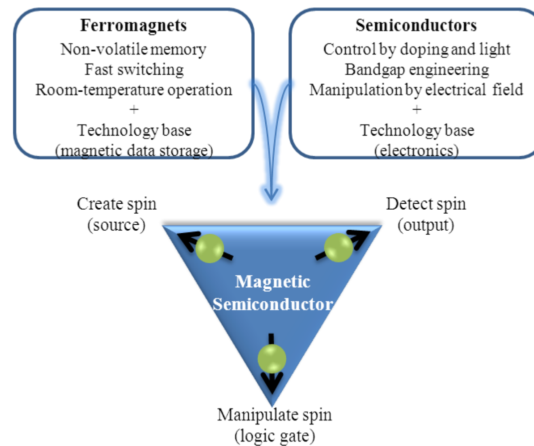

Figure 1: The unique features of ferromagnets and semiconductors (top) are combined in semiconductor spintronics. The cornerstone of semiconductor spintronics, the creation, manipulation and detection of spin polarization, are schematically indicated (bottom).

The goal of this paper is to explore the injection and transport of spins in oxide semiconductors in order to pose ways to enhance or build novel devices with multifunctional functionalities. Thus, in the next section, we briefly describe semiconductor spintronics and presents oxide spintronics in section 3, examining some technologically important oxides used in spintronics and discuss their achievements. Section 4 lays out a discussion on the basic elements of spin injection and transport. Critical studies of spin injection and transport in oxide semiconductor is presented in section 5 while suggestions or recommendations for future applications and/or further research are presented in section 6.

2 SEMICONDUCTORS FOR SPINTRONICS

The quest to develop novel multifunctional spintronic materials and devices resulted in the extensive theoretical and experimental investigations of the new fundamental spin physics and spin-polarized transport in semiconductors. In particular, enormous research activities have been conducted on GaAs [12-15] and silicon

spintronics [16-18] with several key demonstrations and the discovery of exciting new phenomena raising prospects for novel devices having new functionality [12,14]. The first design for a spintronic device based on the metal-oxide-semiconductor technology familiar to microelectronic designers was the field effect spin transistor proposed in 1990 by Datta and Das [19]. This had paved the way for proposals for other devices including spin transistors with several different operating principles [20,21], spin-based diodes [22,23], spin-based field programmable gate arrays [24], dynamic spin-logic circuits [25], spin-only logic [26] and spin communication in silicon [27].

The canonical spin transistor consists of a lateral semiconductor channel with two ferromagnetic contacts (i.e. ferromagnet/semiconductor/ferromagnet sandwich structure), one of which serves as a source of spin-polarized electrons and the other as a detector. Beside the lateral geometry, spin transistors with vertical geometry can also be fabricated. The structure could either be symmetric (i.e. same magnetic material and same tunnel barrier at both interfaces) or non-symmetric (i.e. different magnetic materials and same/different tunnel barriers at the ferromagnet/semiconductor interfaces). In principle, the ferromagnetic electrode could be metallic or semiconducting.

3 OXIDES FOR SPINTRONICS

Oxide spintronics has been extensively studied due to their impressive range of functional properties with high tunability that makes them very important in technological applications. Their transport properties span from superconductivity to high-mobility metallicity, semiconducting properties to insulating behavior and also, ferroic behavior [28]. The progress in thin-film deposition techniques such as pulsed laser deposition (PLD) and molecular beam epitaxy have contributed to the growth of high-quality oxide thin films and heterostructures. This has resulted in the affluence of new physics and novel functionalities that is exhibited by ultrathin oxide films and at the oxide interfaces which complements their use for spintronic devices. Understanding the characteristics or the physics of the materials is key to their use for spintronic applications. Hence, important oxide materials such as MgO, $SrTiO_3$ and LSMO are described, discussing their properties and notable influence on spin transport

3.1 Magnesium Oxide (MgO)

MgO is a crystalline, dielectric and diamagnetic oxide which has a simple rock-salt structure with a lattice parameter of 4.203 Å and a bulk optical band gap of 7.8 eV. It has the ability to generate highly spin-polarized currents. To understand the spin-polarized tunneling in epitaxial or semi-epitaxial tunnel junctions and explore symmetry filtering of the MgO barrier requires the understanding of the band structures of the electrodes and the barrier [30, 31]. The description of the band structure can be considered in two regimes: large tunnel barrier

thicknesses regime and low-thicknesses regime.

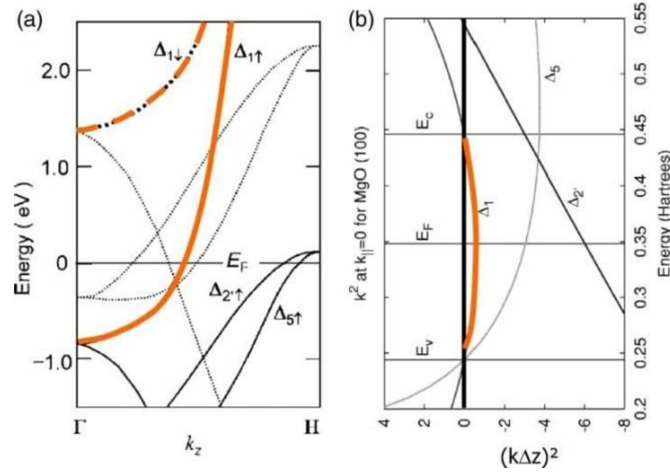

Figure 2: (a) Band structure of b.c.c. Fe in the ΓHdirection corresponding to electron propagating perpendicularly to the interface for majority spin and minority spin states. (b) Complex band structure of MgO in the vicinity of the gap along (100). Negative values of $k^2 = -\kappa$ determine the exponential decay rates for various Bloch states. E_v is the top of the valence band and E_c is the bottom of the conduction band.[30]

The large tunnel barrier thicknesses regime refers to cases in which the tunnel current is carried by states with wave-vector perpendicular to the interface ($k_{\parallel} = 0$). A consideration of the band structure of body-centered cubic (bcc) Fe in the ΓH direction as shown in Figure 2(a) show that at the Fermi level, Bloch states of Δ_1 (spd-like character), Δ_5 (pd-like character) and $\Delta_{2'}$ (d-like character) symmetries coexist for the majority spin electrons while in the minority spin band structure, Δ_1 symmetry is absent. These Bloch states with Δ symmetry decay with different rates in the crystalline MgO barrier. Given that the symmetries of the tunneling waves are conserved, and depending on the dominant tunneling channel or how the Bloch states coupled with the evanescent states, a small or large net spin polarization at the Fermi level can be observed. Butler *et al.* [30] showed that in the parallel configuration, the tunneling is governed by Δ_1 states of majority spin with small decay rate that results in a high conductance state. As shown in Figure 2 (a) Δ_1 decays less than Δ_5, which also decays less than $\Delta_{2'}$ at the Fermi level. Thus, only Bloch states with Δ_1 (high) symmetry dominantly tunnel through the crystalline MgO barrier, with the barrier acting as a symmetry filter. They also showed that in the antiparallel configuration, the current is only due to the transmission of Δ_5 and $\Delta_{2'}$ states with large decay rates since for an injected Δ_1 state, none of the minority Bloch states in the collecting electrode have the correct symmetry and hence the conductance is small.

In the low-thickness regime, the description is less intuitive since contributions of $k_{\parallel} \neq 0$ and interfacial resonance states become significant and affect the conductance in the minority spin channel. The nature of the bonding interface is also found to strongly influence the conductance. For instance, a FeO_x layer at one of the interfaces (i.e. Fe/FeO_x/MgO/Fe) results in a magnitude drop in the TMR due to reduced coupling between the incident majority spin Bloch state of $\Delta_1$symmetry with the MgO evanescent state of the same symmetry [32]

whereas FeO_x layer at both interfaces is predicted to strongly enhance the TMR due to fully coherent tunneling [33]. In asymmetric tunnel junctions, TMR is strongly reduced and oscillate with the MgO thickness as reported by Yuasa *et al*. [34]. Depending on the type of electrode or the coupling between the Bloch states in the electrode and the evanescent states in MgO, large spin polarizations are obtainable resulting in TMR values in excess of 600% at room temperature [35].

3.2 Strontium Titanate ($SrTiO_3$)

$SrTiO_3$ (STO) is also a dielectric and diamagnetic material that crystallizes in the perovskite structure, ABO_3 with an ideal cubic symmetry and a unit cell parameter of $a = 3.905$ Å. It is a band insulator with a bandgap of 3.2 eV [36,37]. As illustrated in Figure 3 (a), the top of the valence band is occupied by O 2p states whereas the conduction band is due to Ti t_{2g} states. Unlike in MgO, the symmetry of the states in the top of the valence band is different from those in the bottom of the conduction band. Calculations of the complex band structure of STO by Bowen *et al*. [38] and Velev *et al*. [39] reveal that there exist Δ_2, $\Delta_{2'}$, Δ_1 and Δ_5 symmetry states. Δ_2 and $\Delta_{2'}$ states are observed to decay very fast compared to Δ_1 and Δ_5 states. Figure 3 (b) shows that the κ loops corresponding to the Δ_1 and Δ_5 symmetry states intersect at energies close to E_F and are accessible in tunneling experiments.

STO is the earliest oxide material to be used in making fully epitaxial tunnel junction with half-metallic mixed valence manganite as electrode. Experimental studies on LSMO/STO/Co tunnel junctions have shown that STO barrier has the ability to reverse the polarity of the spin polarization at the tunnel junctions [40-42]. Other studies with ultrathin Al_2O_3 layer inserted between STO and Co shows that bonding at the interface is important in the determination of the spin polarization [42]. Tunneling and the negative spin polarization observed in LSMO/STO/Co tunnel junction are attributed to metal-induced gap states in the device. Tunnel junctions based on STO and LSMO as electrodes have shown TMR of 1800% at 4.2 K which vanishes at 280 K even though the Curie temperature is 360 K. This effect is attributed to reduced high temperature spin polarization at the interface [43].

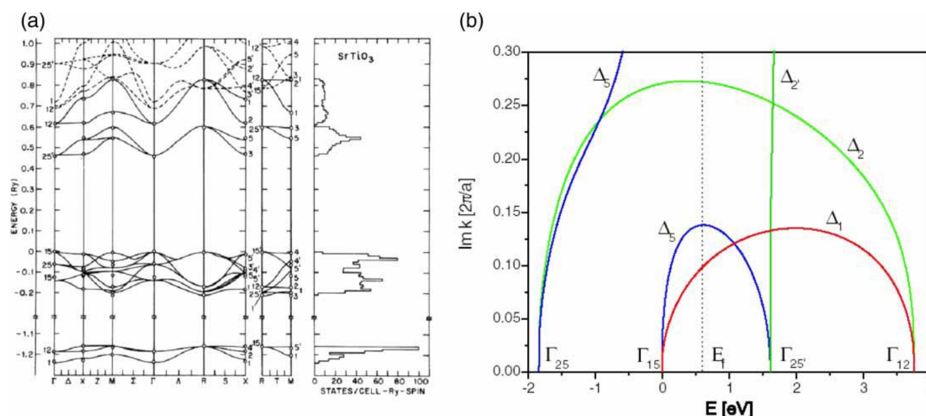

Figure 3: (a) Band structure of SrTiO3 [44]. (b) Complex band structure of SrTiO3 at the $\bar{\Gamma}$ point [39].

While STO is insulating, it becomes semiconducting when doped with niobium (Nb). Nb-doped STO (Nb:STO) is an n-type degenerate semiconductor with a work function of 4.1 ± 0.1 3eV. Its valence band maximum is at 3.1 ± 0.1 3eV and its charge mobility depends on the electron concentration or electron density of the dopant, hence, its properties are tunable. Thus, Nb-doped STO is an unconventional oxide semiconductor with high prospects in spintronic applications.

3.3 Lanthanum Strontium Manganate (LSMO)

Manganites are a class of oxide materials that crystallize in a simple perovskite structure. The parent compound $LaMnO_3$ is an antiferromagnetic charge-transfer insulator. Substituting a fraction of the La^{3+} ions by divalent ions such as Sr^{2+} induces a transition to a ferromagnetic and metallic state for substitution levels of about 17% [45]. Mixed-valence manganite, $La_{1-x}Sr_xMnO_3$ is double exchange half-metallic ferromagnet with a maximum Curie temperature of ~360 K for $x = 0.30 - 0.40$ [45,46] that acts as an excellent spin injector/detector due to near 100% spin polarization at low temperatures.

Optimally-doped $La_{2/3}Sr_{1/3}MnO_3$ (LSMO) was first used as a FM electrode in MTJs with STO barrier by Lu *et al*. and recorded a maximum TMR of 83% at 4.2 K [47] which according to Julliere's formula [6], corresponds to a spin polarization of 54% for the LSMO electrode. Subsequent experimental and theoretical work on MTJs using LSMO as electrode have recorded TMR values corresponding to spin polarization in excess of 90%. This makes LMSO a highly spin-polarized oxide with half-metallic character suitable for use as electrode in spintronic devices. In addition, unlike ferromagnetic metals such as iron, nickel or cobalt, LSMO films are stable against oxidation and therefore immune against any possible degradation of surface magnetization or spin injection efficiency due to oxide formation at the interface.

On the downside, spin polarization decreases with temperature and poor at room temperature. Even though TMR effects decrease rapidly with temperature and disappears at critical temperatures below the Curie temperature, the spin polarization actually does not decay very rapidly with temperature, irrespective of the barrier material. The spin polarization of a manganite free surface however decreases faster with temperature than manganite/barrier interface.

4 BASIC ELEMENTS OF SPIN INJECTION AND TRANSPORT

There are three common aspects of all semiconductor spintronic devices: spin injection, spin transport and spin detection. There are several methods or techniques for spin injection and detection in semiconductors. Some of these are the optical, electrical and resonance methods which are extensively described by Zutic *et al* [4]. Also,

the components of spin transport have been extensively studied in the context of technologically important semiconductors.

4.1 Spin Injection and Detection

The creation of non-equilibrium spin population between the spin-up and spin-down electrons in the conduction band of a semiconductor is termed as spin injection. Four main methods of spin injection have been investigated, which are shown in Figure 4. The first involves using a metallic ferromagnet to inject polarized spins into a semiconductor [19, 48]. The second method entails using a tunneling barrier to reduce impedance mismatches between the ferromagnet and the semiconductor [49]. The third method addresses materialistic mismatches by having the ferromagnetic injector [i.e. dilute magnetic semiconductor (DMS)] itself be semiconducting [50, 51]. The fourth method suggests use of a ferromagnetic tunnel barrier with a non-magnetic metal injector to promote enhanced polarization and efficiency [52,53]. Due to the versatility, stability, and ease of modification, various oxides have been adapted to use in these roles.

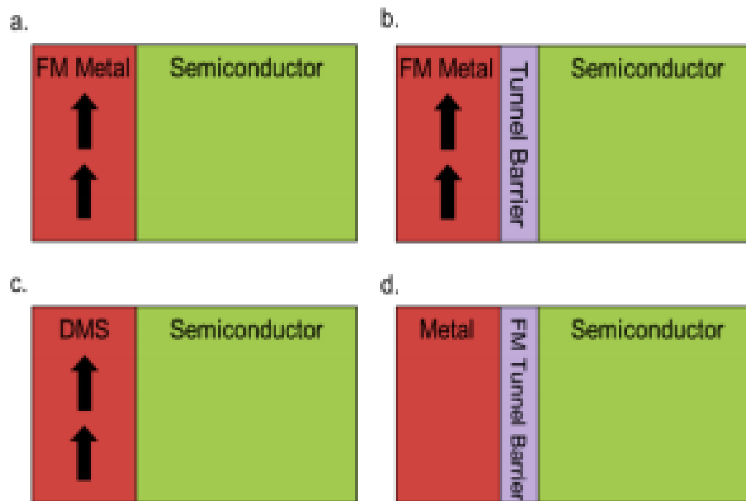

Figure 5. (a) Spintronic device using a ferromagnetic metal and a semiconductor. Theoretically, polarized spin injection should result in a net polarized spin current injected into the semiconductor. (b) Using a half-metal where only one type of spin is present, injection through a tunnel barrier should be ideal. (c) Using a dilute magnetic semiconductor as the means of injection should reduce materialistic mismatches which cause problems in the metal-semiconductor structures. (d) Using a traditional metal, spin polarization can be completed using a dilute magnetic dielectric tunnel barrier, which preferentially allows for tunneling dependent on the spin orientation.

The injection of spin polarized carriers into nonmagnetic metals was first demonstrated experimentally by Johnson and Silsbee [1]. Figure 5 (a) shows the geometry used by them to detect spin accumulation in the nonmagnetic metal. This geometry became very popular as four-terminal non-local (4T- NL) measurement

method of spin accumulation, which alleviates spurious effects in the measurements due to ferromagnetic contacts. Jedema *et al.* provided further evidence for spin injection and detection in metals through precession measurements [54], also called Hanle effect. Conventionally, the Hanle effect is observed by applying and external magnetic field perpendicular to the FM injector's magnetization, in order to drive an incoherent precession of the injected electronic spins, making them precess at a constant angular velocity $\omega_L = g\mu_B B/\hbar$. Electrons traversing from injector to detector acquire a precession angle proportional to the traversal time. At the detector, the spin imbalance is expected to periodically reverse sign, as a function of $B_\perp$. A typical plot of such a measurement is shown in Figure 5 (b).

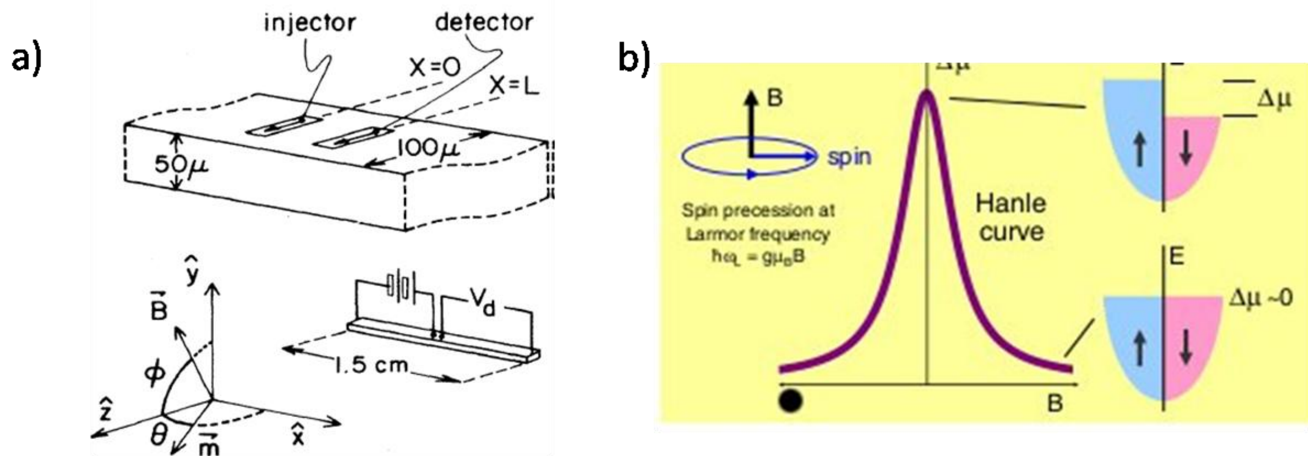

Figure 5. (a) Non-local measurement of spin accumulation in a multi-terminal all-metal spin-valve. (b) Modulation of the output signal V/I due to spin precession as a function of a perpendicular magnetic field $B_\perp$.

4.2 Spin transport

Long spin lifetimes and coherent spin transport in semiconductor systems and thin film heterostructures are of primary concern to the spintronics field. In addition, long spin-diffusion/relaxation length, large resistance-area (RA) product, i.e. large insulating/barrier resistance are relevant in realizing efficient spintronic devices. Another important aspect of this field is spin manipulation which is exercised during spin transport to modify spin polarization to achieve desirable terminal (I-V) characteristics. It is worth noting that the spin polarized carriers in a semiconductor do not retain their polarization for indefinite amount of time due to spin relaxation from various spin-scattering mechanisms.

Spin Relaxation

After the injection, the spin polarized carriers travel through the paramagnetic semiconductor under the influence of a transport-driving electric field. During their transit, different spins interact with their environments differently (spin-orbit, hyperfine and carrier-carrier interactions) and their original orientations get changed by

various amounts. The magnitude (P) of the ensemble spin polarization decreases with time (t) as well as with distance (x) measured from the injection point. This gradual loss in magnitude of the injected spin polarization is termed as *spin relaxation*. Assuming an exponential decay, spin relaxation/diffusion length L_s (or spin relaxation/diffusion time τ_s) is defined as the distance (or duration) over which the spin polarization reduces to 1/e times its initial value. For $L \gg L_s$ (or $t \gg \tau_s$), $P \rightarrow 0$, implying complete loss of spin polarization. In other words, spin relaxation phenomenon in the paramagnet tends to bring the non-equilibrium spin polarization back to equilibrium non-polarized condition. Since the underlying philosophy is to exploit the non-zero spin polarization, one always attempts to suppress spin relaxation and enhance spin relaxation length and time in the paramagnetic semiconductor. If the spins of all carriers change in unison, then the magnitude of the ensemble spin polarization will remain the same but its orientation will change. In this case spin relaxation is suppressed. A standard method to extract spin relaxation length (L_s) and spin relaxation time (τ_s) in a paramagnetic material is to perform a spin-valve experiment. A spin-valve is a trilayered construct, in which the paramagnetic material of interest is sandwiched between two ferromagnetic electrodes of different coercivities

There are several mechanisms in solid that are responsible for spin relaxation. For example, in semiconductors and metals, the most dominant mechanisms are (a) Elliot-Yafet mechanism in which the electrons scattering off impurities or phonons have a tiny chance to flip its spin at each scattering; (b) D'yakonou-Perel mechanism in which electron spins precess along a magnetic field which depends on the momentum. At each scattering, the direction and the frequency of the precession changes randomly; (c) Bir-Aronov-Pikus mechanism in which electrons exchange spins with holes which then lose spins very fast due to the Elliot-Yafet mechanism; and (d) hyperfine interaction with nuclei. Among these, the first two mechanisms accrue from spin-orbit interaction. The third one originates from exchange coupling between electron and hole spins, and the last is due to interaction between carrier spins and nuclear spins. Detailed descriptions of these mechanisms are presented by Zutic *et al.* [4].

5 SPIN INJECTION AND TRANSPORT IN OXIDE SEMICONDUCTORS

As mentioned in previous sections, oxides possess impressive range of functionalities with high tunability that make them ideal for investigation of spin or electron transport and are very important in technological applications. For the purpose of this work, we focus on spin injection and transport in the n-type oxide semiconducting Nb-doped $SrTiO_3$ (Nb:STO).

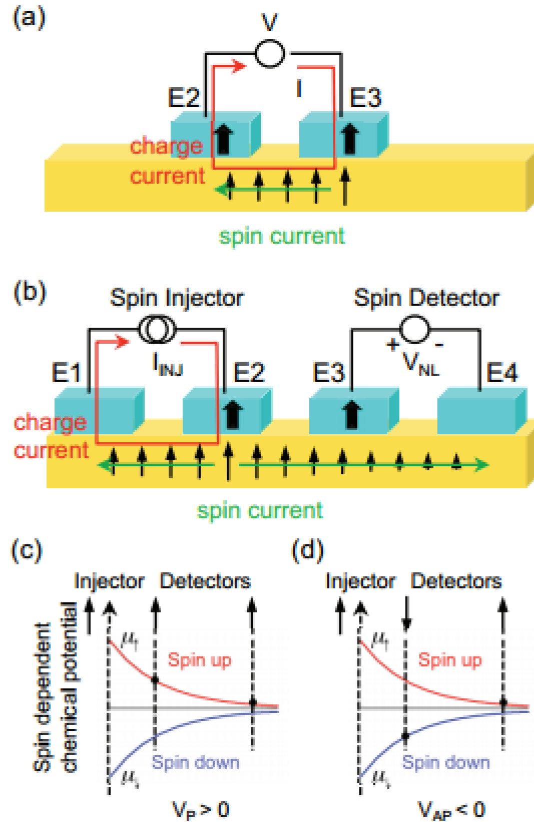

Figure 6. The spin transport measurement. (a) schematic of local spin transport measurements. (b) schematic of nonlocal spin transport measurements. (c-d) spin dependent chemical potential for parallel and anti-parallel states of spin injector and detectors in the nonlocal geometry.

When a thin epitaxial film of LSMO is grown on Nb:STO substrate it forms a diode with a Schottky barrier at the interface which is sensitive to the interface electronic states [55]. Typically, there are two geometries for electrical spin transport measurements. First is the conventional spin transport geometry, known as the "local" (3T) measurement, which measures the resistance across two ferromagnetic electrodes [Figure 6(a)]. Spin polarized electrons are injected from one electrode, transported across the semiconductor (Nb:STO), and detected by the second electrode. The spin transport is detected as the difference in resistance between the parallel and anti-parallel magnetization alignments of the two electrodes. This is the geometry used for magnetic tunnel junctions and current-perpendicular-to-the-plane giant magnetoresistance (CPP-GMR) mentioned earlier. The second geometry is the "nonlocal" measurement which uses four electrodes, as shown in Figure 6(b). Here, a current source is connected across electrodes E1 and E2 to inject spins at E2. For spin detection, a voltage is measured across electrodes E3 and E4, and the signal is due to the transport of spins from E2 to E3. This measurement is called "nonlocal" because the voltage probes lie outside of the current loop. After the spin injection, the spins at E2 are able to diffuse in both directions, toward E1 (as a spin current with charge current) and toward E3 (as a spin current without charge current). This spin diffusion is usually described by a spin

dependent chemical potential ($\mu_{\downarrow}$ and $\mu_{\downarrow}$) where a splitting of the chemical potential corresponds to the spin density in the semiconductor. Figures 6(c) and 6(d) show that as the spins diffuse toward E3, the spin density decays due to spin flip scattering. Thus, the voltage will be positive for the parallel alignment of E2 and E3 ($V_P > 0$, Figure 6(c), black dots) and negative for the antiparallel alignment ($V_{AP} < 0$, Figure 6(d), black dots). The signal generated by the spin transport is the nonlocal magnetoresistance (MR), defined as $\Delta R_{NL} = (V_P - V_{AP})/I$, where I is the injection current. Like most ferromagnet/semiconductor (FM/SC) devices, the injection of spin-polarized electrons from the half-metallic LSMO into the oxide semiconductor has been demonstrated by electrical, optical, ballistic electron emission microscopy (BEEM) and vacuum tunneling methods.

To investigate the electron transport properties across the oxide heterointerface of LSMO/Nb:STO, various methods such as the conventional current-voltage (I-V), capacitance-voltage (C-V) and Internal Photoemission (IPE) that are used to study transport properties in non-oxide materials can be employed. In addition, complementary techniques such as BEEM which compensates the limitations of the conventional techniques in investigating for example, the influence of interface states and interface dipoles, temperature and electric field dependence of dielectric permittivity has also been used to probe the charge/spin transport properties of hot electrons in the oxides [57,58].

It is worth noting that very little is known about electron transport in oxide heterointerfaces with transition-metal oxides. In order to probe vertical transport of hot electrons across the LSMO/Nb:STO and quantify the transport parameters, Rana *et al*. [58] made use of the current-perpendicular -to-plane (CPP) configuration and the BEEM technique. With this configuration and technique, unpolarized electrons are injected from the STM (Scanning Tunneling Microscope) tip perpendicular to the device layers through a thin tunnel barrier at typical energies of 0.6-2 eV above the Fermi energy into the base where transport and attenuation occur as a result of scattering processes and propagation. Energy dependence of hot electron transmission in LSMO for different LSMO thicknesses and tunnel current are investigated at room temperature. The BEEM transmissions are found to decrease with increasing LSMO thickness and decreasing tunnel current and the hot electron attenuation length in LSMO is found to increase from 1.48 ± 0.10 u.c. (unit cell) at – 1.9 eV to 2.02 ± 0.16 u.c. at -1.3 eV. The experimental methods based on hot electron transport in a vertical device structure provides a measure of the attenuation length and paves the path for further investigations to advance the field of oxide electronics.

6 CONCLUSION

We have analyzed semiconductor spintronics and critically reviewed some technologically important oxides that are use in spintronic applications. Spin injection and transport in semiconductors and particularly in oxide semiconductors are described. Review of spin/charge transport in oxide semiconductors reveals the many physical properties that need to be explored and mechanisms that need understanding. Among these are defect

states and interface effects.

The prospects of oxide semiconductors add to the indication that spintronics devices may hold the key to advancing the computing power of electronics long beyond the limitations of Moore's law. Although semiconductor spintronics has witnessed huge progress in recent years, oxides will provide an important role in this advancement due to their capacity to fulfill any role in a spintronics device. By achieving a better understanding of oxide systems and further improving current oxide capabilities, spintronics technologies have the potential to transition from the laboratory to full-scale production in the near future.

REFERENCES

1. M. Johnson and R. H. Silsbee, *Physical Review Letters* **55** 1790 (1985)
2. M. N. Baibich, J.-M. Broto, A. Fert, F. Nguyen Van Dau, F. Petroff, P. Eitenne, G. Creuzet, A. Friedrich, and J. Chazelas, *Physical Review Letters* **61**, 2472 (1988).
3. Binasch, G., Grunberg, P., Saurenbach, F., Zinn, W., *Physical Review B* **39**, 4828 (1989).
4. Žutić, I., Fabian, J. and Das Sarma, S., *Rev. Mod. Phys*. **76**, 323 (2004).
5. R. Meservey, P. M. Tedrow, *Physics Reports* **238**, 173 (1994).
6. M. Julliere, *Physical Letters A* **54(3)**, 225 (1975).
7. C. Chappert, A. Fert, & F. Nguyen van Dau, *Nature Mater.* **6,** 813 (2007).
8. S. Yuasa & D. D. Djayaprawira, *J. Phys. D* **40,** R337 (2007).
9. A. Fert, *Rev. Mod. Phys.* **80,** 1517 (2008).
10. Das *et al*, *American Scientist* **89**, 516 (2001).
11. Ron Jansen, *Nature Mater.* **11**, 400 (2012).
12. D.D. Awschalom and M.E. Flatté, *Nature Phys*. **3**, 153 (2007).
13. Žutić, I., Fabian, J. & Das Sarma, *Rev. Mod. Phys*. **76**, 323 (2004).
14. J. Fabian, A. Matos-Abiague, C. Ertler, P. Stano & I. Žutić, *Acta Phys. Slov*. **57**, 565 (2007).
15. Wu, M. W., Jiang, J. H. &Weng, M. Q. *Phys. Rep*. **493**, 61 (2010)
16. Appelbaum, I., B. Huang, and J. Monsma, *Nature* **447**, 295 (2007).
17. Huang, B., D. Monsma, and I. Appelbaum, *Phys. Rev. Lett.* **99**, 177209 (2007).
18. Huang, B., D. Monsma, and I. Appelbaum, *Appl. Phys. Lett*. **91**, 072501 (2007).
19. Datta, S. and Das, B., *Appl. Phys. Lett.***56**, 665 (1990).
20. Flatté, M. E., Yu, Z. G., Johnston-Halperin, E. and Awschalom, D. D., *Appl. Phys. Lett.* **84,** 4740 (2003).
21. Fabian, J., Žutić, I. and Das Sarma, S. *Appl. Phys. Lett.* **84,** 85 (2004).
22. Flatté, M. E. and Vignale, V. *Appl. Phys. Lett.* **78,** 1273 (2001).
23. Castelano, L. K. and Sham, L. J. *Appl. Phys. Lett.* **96,** 212107 (2010).
24. Tanamoto, T. *et al. J. Appl. Phys.* **109,** 07C312 (2011).
25. Dery, H., Dalal, P., Cywiński, L. and Sham, L. J. *Nature* **447,** 573 (2007).
26. Behin-Aein, B., Datta, B., Salahuddin, S. and Datta, S. *Nature Nano.* **5,** 266
27. Dery, H., Song, Y., Li, P. and Žutić, I. Appl. Phys. Lett. 99, 082502 (2011).
28. Bibes, M. et al., *Advances in Physics* **60**, 5 (2010).
29. Lou, Y. et al., *Phys. Rev. B*, *Condens. Matter,* **54**, R8357 (1996).
30. Butler, W.H., Zhang, X.G.,Schulthess, T.C. and MacLaren, J.M. *Phys. Rev. B* **6**, 054416 (2001).
31. Mathon, J.and Umerski, A., *Phys. Rev. B* **63**, 220403(2001).
32. X.G. Zhang,W.H. Butler, and A. Bandyopadhyay, *Phys. Rev. B* **68** 092402 (2003).

33. C. Tusche, H.L. Meyerheim, N. Jedrecy, G. Renaud, A. Ernst, J. Henk, P. Bruno, and J. Kirschner, *Phys. Rev. Lett*. **95,** 176101 (2005).
34. S.Yuasa, A. Fukushima, T. Nagahama, K. Ando, and Y. Suzuki, *Jpn. J.Appl. Phys*. **43,** L588 (2004).
35. S. Ikeda, J. Hayakawa,Y. Ashizawa,Y. Lee, K. Miura, H. Hasegawa, M. Tsunoda, F. Matsukura, and H. Ohno, *Appl. Phys. Lett*. **93** 082508 (2008).
36. K. Benthemvan, C. Elsasser, and R.H. French, *J. Appl. Phys*. **90,** 6156 (2001).
37. D. Kan, T. Terashima, R. Kanda, A. Masuno, K. Tanaka, S. Chu, H. Kan, A. Ishizumi, Y. Kanemitsu, Y. Shimakawa and M. Takano, *Nature Mater*. **4** 816 (2005).
38. M. Bowen, A. Barthélémy, V. Bellini, M. Bibes, P. Seneor, E. Jacquet, J.P. Contour, and P.H. Dederichs, *Phys. Rev. B* **73** 140408 (2006).
39. J.P. Velev, K.D. Belashchenko, D.A. Stewart, M. Schilfgaardevan, S.S. Jaswal, and E.Y. Tsymbal, *Phys. Rev. Lett.* **95** 216601 (2005).
40. J.M. De Teresa, A. Barthélémy, A. Fert, J.P. Contour, R. Lyonnet, F. Montaigne, P. Seneor, and A. Vaurès, *Phys. Rev. Lett.* **82** 4288 (1999).
41. I.J. Vera Marún, F.M. Postma, J.C. Lodder, and R. Jansen, Phys. Rev. B 76 (2007), p. 064426.
42. J.M. De Teresa, A. Barthélémy,A. Fert, J.P. Contour, F. Montaigne, and P. Seneor, *Science* **286** 507 (1999).
43. Bowen, M., M. Bibes, Barthélémy, A., Contour, J.-P., A. Anane, Y. Lemaıˆ-tre, and A. Fert, *Appl. Phys. Lett.* **82**, 233 (2003).
44. L.F. Mattheiss, *Phys. Rev. B* **6** 4718 (1972),.
45. Imada, M., Fujimori, A., and Tokuro, Y., *Rev. Mod. Phys*., **70**, 1039 (1998).
46. J. Coey, M. Viret, and S. von Molnr, *Adv. in Phys.*, **48**, 167 (1999).
47. Y. Lu, W. Li, G. Gong, G. Xiao, A. Gupta, P. Lecoeur, J. Sun, Y. Wang, and V. Dravid, *Phys. Rev. B*, **54**, R8357 (1996).
48. Johnson, M. *IEEE Spectrum*, **31**, 47 (1994).
49. Rishton, S.A. Lu, Y. Altman, R.A. Marley, A.C. Bian, X. P. Jahnes, C. Viswanathan, R. Xiao, G. Gallagher, W.J. Parkin, S.S. P. *Microelectron. Eng*., **35**, 249 (1997).
50. Ohno, H. *Science*., **281**, 951 (1998).
51. M. Snure, D. Kumar, A. Tiwari, *JOM*., **61**, 72 (2009).
52. A. Tiwari, V.M. Bhosle, S. Ramachandran, N. Sudhakar, J. Narayan, S. Budak, A. Gupta, *Appl. Phys. Lett*., **88**, 142511 (2006).
53. B. Vodungbo, Y. Zheng, F. Vidal, D. Demaille, V. H. Etgens, D.H. Mosca, *Appl. Phys. Lett*., **90**, 062510 (2007).
54. F. J. Jedema, H. B. Heersche, A. T. Filip, J. J. A. Baselmans, and B. J. van Wees, *Nature* **416**, 713 (2002).
55. [56] G. Schmidt, D. Ferrand, L. W. Molenkamp, A. T. Filip, and B. J. van Wees, *Physical Review B*, **62**, R4790 (2000).

56. [57] S. Parui, K. G. Rana, and T. Banerjee. *Electron Devices Meeting (IEDM), IEEE International*. *IEEE,* 11.4 1-11(2012).
57. [58] K. G. Rana, *et al*. *Scientific reports* **3,** 1274 (2013).